Superelevation Transition Assessment on Rural Roads with Reverse Consecutive Horizontal Curves

Stergios Mavromatis
School of Civil Engineering
National Technical University of Athens, Greece, GR-15773
e-mail: stemavro@central.ntua.gr

Vassilios Matragos
School of Civil Engineering
National Technical University of Athens, Greece, GR-15773
e-mail: vasmatragos@mail.ntua.gr

Konstantinos Apostoleris
School of Rural and Surveying Engineering
National Technical University of Athens, Greece, GR-15773
e-mail: kapostol@central.ntua.gr

Sophia Vardaki
School of Civil Engineering
National Technical University of Athens, Greece, GR-15773
e-mail: sophiav@central.ntua.gr

George Yannis
School of Civil Engineering
National Technical University of Athens, Greece, GR-15773
e-mail: geyannis@central.ntua.gr

Word Count: 4052 words + 2 tables (250 words per table) = 4552 words

Submitted February 2020

ABSTRACT
The design of consecutive reverse horizontal curves is a common practice in road design with many environmental and economic benefits. In order the driver to avoid instantaneous lateral acceleration variation during the curvature direction shifting; nearly all design guidelines adopt spiral curves between the opposite turning directions. During the design of such curves, most European road design guidelines treat the spiral curves on both sides of the reverse curvature point (point where end of spiral on first curve concurs with beginning of spiral on second curve), as the boundaries within where the necessary superelevation transition takes place as well. Through this concept, the point with level (horizontal) superelevation rate usually coincides with the point of reverse curvature, thus creating a breakpoint at the superelevation transition when the reverse curves have different either superelevation values or spiral lengths. The paper investigates the impact of utilizing a continuous (linear) superelevation transition between the points where the first circular curve ends and the second circular curve begins. This assessment is carried out by quantifying the safety margins in terms of demanded friction values for both approaches. The investigation was based on the German RAL, 2012 design guidelines, tailored for unfavorable cases of high superelevation demand (sharp curves), through the utilization of an existing vehicle dynamics model. The analysis, revealed that the vehicle undergoes an immediate but rather moderate lateral friction demand variation. However, before introducing the proposed approach in road design practice, there are certain issues that necessitate further research.
Keywords: Reverse Horizontal Curves, Superelevation Transition, Side Friction

INTRODUCTION AND PROBLEM STATEMENT

Road layouts with consecutive reverse horizontal curves consist a common practice in road design. Although the proper design of such arrangements offers many environmental and economic benefits, reverse horizontal curves impose numerous safety issues to overcome. For example, besides sight distance limitations, drivers experience difficulties to sustain their vehicle inside the driving lane due to the direction swap of the centrifugal force.

Excessive centrifugal force generated by high design speed values, or sharp horizontal curvature, may cause abrupt, uncomfortable and unsafe maneuvers, or even lateral drifting of the vehicle. The effect of such unfavorable conditions can be reduced from the superelevation requirement, which is critical in terms of counterbalancing the instantaneous lateral acceleration variation caused by the centrifugal force during the curvature direction shifting.

Although lateral friction force developed between the tires and road surface interaction also assists such a counterbalance of the lateral acceleration, in order a vehicle during the negotiation of horizontal curves to optimize the reduction impact of the centrifugal force, it is very important the outer to the curve edge-line of the pavement to be the superelevated one; higher than the one inside.

Figure 1(a,b) shows a simplification of the lateral force distribution during a right turned curve applied on the well know mass-point, widely accepted in road design for the determination of the minimum horizontal radius (e.g. 1, 2, 3, 4).

During the lateral equilibrium, the following Equation applies:

$$\frac{mV^2}{R}\cos e = mg\sin e + S \quad (1)$$

$$\rightarrow \frac{mV^2}{R}\cos e = mg\sin e + f_R(mg\cos e + \frac{mV^2}{R}\sin e) \quad (2)$$

Assuming that ($e << \rightarrow \cos e \approx 1,\ \sin e \approx e$)

$$\rightarrow \frac{V^2}{gR} = \frac{e+f_R}{1-ef_R} \approx e + f_R \quad (3)$$

$$\rightarrow R_{min} = \frac{V^2}{g(f_R+e)} \quad (4)$$

where:
g: gravitational constant ($g=9.81 m/sec^2$)
m: vehicle mass (kgr),
e: superelevation rate (%/100)
V: vehicle speed (m/sec),
R: curve horizontal radius (m),
S: lateral friction force (N),
f_R: lateral friction coefficient

From Equation 4 it can be seen that the use of superelevation allows a vehicle to travel through curves more safely, since there is a safety margin either to increase speed or to reduce the curve radius by maintaining the alignment and vehicle speed respectively.

Therefore, between succeeding reverse circular curves, in order the superelevation to be designed in accordance with Figure 1, many design guidelines (e.g. 1, 2, 3, 4) request an adequate tangent length between, or preferably, an equivalent length with spiral curves.

Spiral curves provide gradual change on the centrifugal force as well as more comfortable alignment between tangents and circular curves. More specifically in the AASHTO, 2018 design guidelines (1) it is stated that transition (spiral) curves simulate the natural turning path of a

vehicle, minimize encroachment on adjoining traffic lanes and tend to promote uniformity in speed.

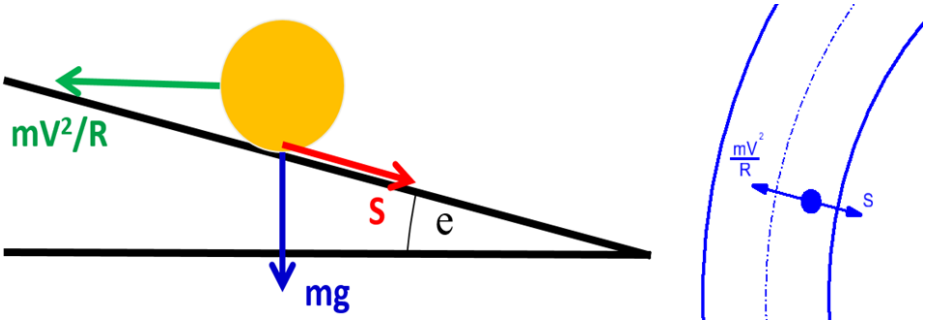

(a) lateral direction of travel (b) plan view

Figure 1(a,b) Lateral Force Distribution during a Right Turned Curve on the Point-Mass Model.

During the design of consecutive curves, most European road design guidelines (e.g. 2, 3, 4) treat the spiral curves on both sides of the reverse curvature point (point where end of spiral on first curve concurs with beginning of spiral on second curve), as the boundaries within where the necessary superelevation transition takes place as well.

Through this conventional approach, the point with level (horizontal) superelevation rate usually coincides with the point of reverse curvature. As far as the two opposite curves have the same superelevation rates and spiral lengths the rotation rate of the superelevated pavement transition within the spiral curves is uniform (continuous). However, in case the reverse curves have different superelevation rates or spiral lengths, a breakpoint of the rotation rate is created at the point of reverse curvature. Such a case, where the reverse curve is formed by left curve 1 and right curve 2 (Figure 2a), is shown through Figure 2b.

The paper investigates the impact of generalizing a continuous superelevation transition (rotation rate) between the points where the first circular curve ends and the second circular curve begins for arrangements of reverse curves. Such an alternative approach simplifies the superelevation rotation process as is far more construction-friendly. This assessment is performed by quantifying the safety margins in terms of demanded friction values for both conventional and continuous approaches, utilizing an existing vehicle dynamics model.

(a) reverse curve alignment projected linearly

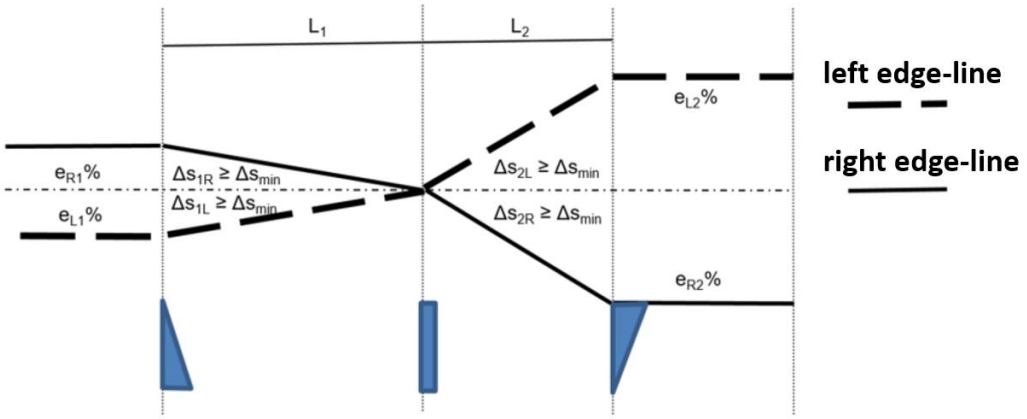

(b) superelevation transition

Note. (i=1,2): R_i, A_i, L_i : curve i radius, spiral parameter and spiral length (m). e_{Li}, e_{Ri}, Δs_{iL}, Δs_{iR}: curve i left and right superelevation rates and superelevation rotation rates (%).
Δs_{min}: minimum superelevation rotation rate (%).

Figure 2(a,b) Superelevation rotation breakpoint at the point of reverse curvature.

METHODOLOGY

The proposed investigation is based on a realistic representation of the forces acting on a moving vehicle during tangent and curved alignments. Such an investigation has already been addressed in previous research of the authors (5-7) where aiming to assess vehicle safety from the interaction between road geometry, tire - pavement friction and vehicle parameters, a vehicle dynamics model was developed. The following sub-section provides a brief discussion on how the model was structured, where more details regarding the full equations description as well as the model's validation process are available through references (5-7).

Vehicle Dynamics Approach

All forces and moments applied to the vehicle were analyzed into a moving three-dimensional coordinate system, coinciding at the vehicle gravity center and formed by the vehicle's longitudinal (X), lateral (Y) and vertical (Z) axis respectively. The vehicle's coordinate system applied for a front wheel driven (FWD) vehicle is shown in Figure 3. Through these axes, the impact of certain vehicle technical characteristics, road geometry and tire friction were expressed, such as: vehicle speed/ wheel drive/ sprung and unsprung mass and it's position of gravity center/ aerodynamic drag/ vertical lift/ track width/ wheel-base/ roll center/ suspension roll stiffness/ cornering stiffness/ grade/ superelevation rate/ rolling resistance tire-road adhesion values and horsepower supply.

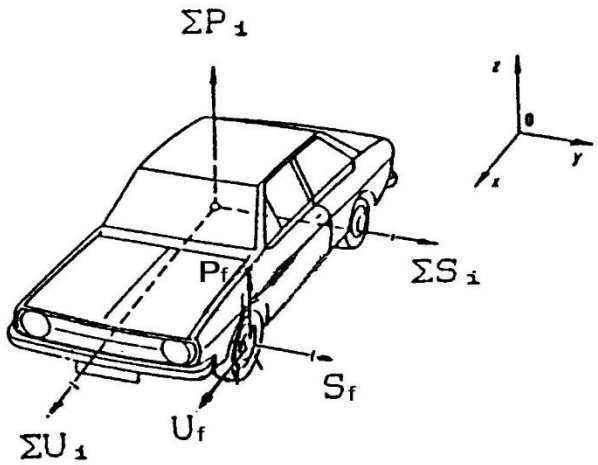

Note: Ui (longitudinal forces); Si (lateral forces); Pi (vertical forces); U_f, S_f (forces in front axle)

Figure 3 Vehicle Coordinate System

Moreover, the model takes into account variables related to vehicle steering and tire sideslip angles (8), the actual wheel load due to the lateral load transfer as well as the corresponding alteration of the lateral force on each wheel, thus creating a four-wheel vehicle dynamics modelling (8-10).

The available tractive effort of the vehicle (driving force minus rolling resistance) acting on the front or rear axle (depending on the driving configuration) was associated to the vehicle's speed as well as the net power available at the driving wheels. Since a vehicle cannot always be driven at 100% of its available horsepower rate, the horsepower utilization factor (n) was introduced and the following equation applies:

$$Fx = 745.60 \frac{P}{V} \frac{n}{100} \quad (5)$$

where :

F_x : tractive force (Nt)

P : net engine horsepower available at the driven axle [around 94% of the nominal value, (11)] (hp)

v : vehicle speed (m/sec)

n : horsepower utilization factor (%)

By applying laws of mechanics, the vehicle's instant acceleration, which is expressed as a four-degree polynomial equation, can be formed as a function of vehicle's instant speed as well as driven distance, thus delivering the following differential equation which is resolved by utilizing numerical Runge-Kutta method (12):

$$a(v) = \frac{dv}{dd} v \quad (6)$$

where:

a(v): acceleration (m/sec^2)

v: speed (m/sec)

d: distance (m)

The solution of Equation (6) delivers the vehicle speed variation as a function of the driven distance.

On the other hand, according to (13), pavement friction reserves are distributed to the longitudinal and lateral direction of travel. During a curve negotiation, the portion of friction experienced in the longitudinal direction, is engaged by the friction demanded laterally and the following equation applies, the upper limit of which is known as impending skid conditions:

$$\left(\frac{f_T}{f_{T,max}}\right)^2 + \left(\frac{f_R}{f_{R,max}}\right)^2 \leq 1 \qquad (7)$$

where :

f_T : longitudinal friction demand

$f_{T,max}$: maximum longitudinal friction

f_R : side friction factor

$f_{R,max}$: maximum side friction

Assuming a desired steady state vehicle cornering speed, referring to certain vehicle, road and friction parameters, by forcing a(v)=0 (Equation 6) and based on Equation 5, the model's software calculates the horse-power utilization factor (n). At the same time, the demand in longitudinal and side friction is calculated and vehicle's potential skidding is checked through Equation 7.

It is evident that the sliding friction coefficient and consequently the relevant peak friction values in both directions are subject to marginal variations in terms of wet-dry pavement conditions as well. For this reason, in the present study the value of peak friction coefficients examined were set to 0.30 in order to address wet pavements with poor friction performance.

Road and Vehicle Parameters

The investigation regarding continuous superelevation rotation rate between the end of the first circular curve and the beginning of the second, is performed for the German rural design guidelines RAL 2012 (2). The assessment is based on the critical situation according to which the continuous rotation rate delivers negative superelevation on rather sharp circular curve. Therefore, EKL 3 design class was selected, the control values of which are shown in Table 1.

TABLE 1 Control Values for EKL 3 Design Class (RAL, 2012)

Design Speed V (km/h)	Radius R_{min} (m)	Spiral Parameter A_{min} (m)	Superelevation e_{max} (%)	Rotation Rate Δs_{min} (%)	Grade s_{max} (%)
90	300	R/3	7	0.35	6.50

Regarding vehicle parameters, a C-class mid-sized, front wheel drive (FWD) passenger car was selected, where at least from the vehicles' dimensions' points of view, a real case is represented (KIA Proceed). Although an effort was made to provide the utilized vehicles' parameters from the vehicle industry, most of them were taken from the literature (9). The vehicle parameters inserted in the vehicle dynamics model are shown in Table 2.

TABLE 2 Vehicle Parameters Inserted to the Model

L (m)	wheelbase
t_f (m)	front track width
t_r (m)	rear track width
m (kgr)	vehicle mass
l_f (m)	position of gc from front axle
h (m)	position of gc from surface
$K_{\varphi f}$ (Nm/rad)	suspension roll stiffness (front)
$K_{\varphi r}$ (Nm/rad)	suspension roll stiffness (rear)
C_{af} (kp/rad)	cornering coef. (front)
C_{ar} (kp/rad)	cornering coef. (rear)
m_{uf} (kgr)	unsprung mass (front)
m_{ur} (kgr)	unsprung mass (rear)
h_{Rf} (m)	roll center height (front)
h_{Rr} (m)	roll center height (rear)
r_{dyn} (m)	dynamic radius (tire)
A_f (m^2)	frontal area
c_N	lift drag
c_d	aerodynamic drag
P (hp)	hp available on wheels

ANALYSIS

As already stated above, the objective of the present research is to assess an alternative and more construction-friendly process for superelevation transition between consecutive reverse horizontal curves. More specifically, the paper investigates the potential of introducing a continuous rotation rate between the end of the first circular curve and the beginning of the second, against the existing approach according to which the superelevation transition is formed through a breakpoint at the point of reverse curvature (level superelevation, e=0).

Figure 4 shows once again a left-to-right reverse curve arrangement (curve 1 to curve 2 respectively), where certain graphs provide more details regarding the performed assessment.

The bottom graph of Figure 4 shows a linear projection of the reverse curve alignment at the area of the spiral curves. The chainage of the ending point of the first circular curve R_1, which coincides with the beginning of the first spiral curve (A_1) was set to 0.

The following graph upwards shows the superelevation rotation rates (Δs_i) of the left edge-line between the two reverse circular curves. More specifically, the conventional (applied in current practice) superelevation rotation rate approach is shown against the continuous (proposed). The typical approach is formed of two different superelevation rotation rates Δs_{1L} and Δs_{2L} respectively, shown with two blue lines, and correspond to the superelevation variation regarding the two spiral curves with parameters A_1 and A_2. On the other hand, the continuous superelevation rotation rate (Δs) is shown with red line.

A closer look on the proposed superelevation transition of Figure 4 reveals the following three sections:

- length of spiral curve 1 (left-curved) where the superelevation rotation rate in terms of curve rotation delivers (section 1):
    - positive superelevation for the conventional approach which varies between the ending point of the first circular curve (e_{L1}) and 0% (e_{L1} is positive in terms of curve rotation but its value is negative, since the left edge-line is below the axis rotation)
    - positive superelevation for the continuous approach which varies between e_{L1} and e_{x1} (e_{x1} represents the equivalent superelevation rate for the continuous approach at the reverse curvature point and has negative value for the same reason mentioned above)
- segment of spiral curve 2 (right curved) where the superelevation rotation rate in terms of curve rotation delivers (section 2):
    - positive superelevation for the conventional approach which varies between 0% and e_{x2} (e_{x2} represents the equivalent superelevation rate for the conventional approach at the point where the superelevation rate for the continuous approach is 0% and has positive value, since the left edge-line is above the axis rotation)
    - negative superelevation for the continuous approach which varies between e_{x1} and 0%
- remaining segment of spiral curve 2 (right curved) where the superelevation rotation rate in terms of curve rotation delivers (section 3):
    - positive superelevation for the conventional approach which varies between e_{x2} and e_{L2}
    - positive superelevation for the continuous approach which varies between 0% and e_{L2}

It is evident that potential critical situations of the assessment must be investigated at the starting area of the right curve (beginning of section 2), where the continuous superelevation rotation rate approach is superelevated negatively in terms of curve rotation. Therefore, the absolute value of e_{x1} must be maximized and the same time A_1 minimized. In other words, the investigation should be performed on rather sharp circular curves. This explains the reason why EKL 3 design class was utilized (R was set to 300m, A_1 was set to R/3=100m, and e_{Li} for both circular curves was set to 7.0%).

It should also be mentioned that the superelevation rotation rates (Δs_i) were drawn in order to be always greater than Δs_{min}=0.35%.

Within a spiral curve (with parameters A, R), the formula describing the superelevation rotation rate Δs_i is as follows:

$$\Delta s_i = \frac{e_2 - e_1}{A^2} Rb \qquad (8)$$

where:

e_1: superelevation rate at the beginning of the spiral curve (%)

e_2: superelevation rate at the end of the spiral curve (%)

b: lateral distance between outer point of traffic lane and rotation axis (3.50m for EKL 3) (m)

Therefore, the lowest Δs (Δs_{2L}) was set to 0.35%, where through Equation 8, the spiral parameter A_2 was determined (A_2=145.00m).

Figure 4 further shows the demanded side friction values (f_R) for both approaches. More specifically, it can be seen that at the circular curves area, since the radii values and superelevation rates are equal, the delivered f_R values are equivalent.

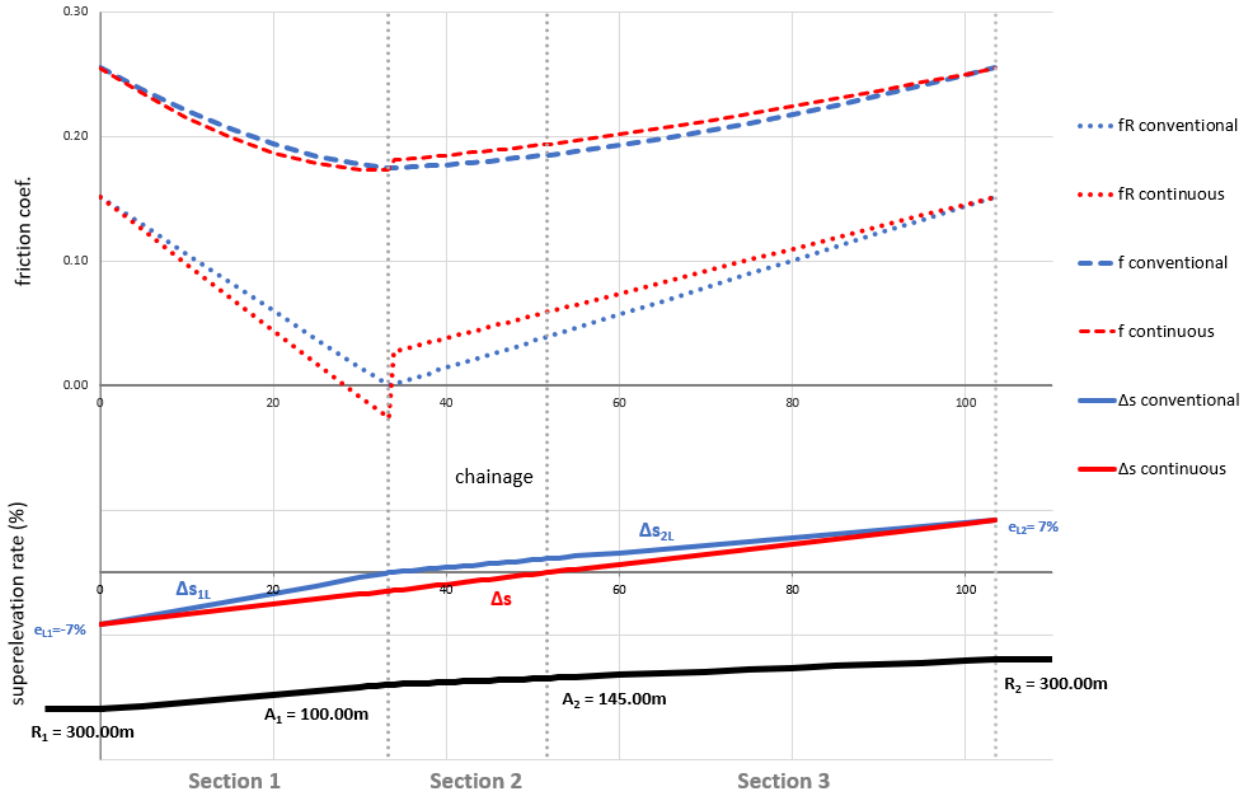

Figure 4 Demanded Side Friction Values (f_R) for Both Approaches

However, this is not the case inside the transition curves. At the area of section 1, the superelavation rates of the continuous approach are higher, where as a result the demanded lateral friction values are somehow lower. Within section 3, the opposite phenomenon is reported.

The most interesting finding can be seen at the area surrounded by section 2, and more specifically at the breakpoint area where the curve changes direction from left to right. At that point, the conventional superelevation rotation rate approach has no demand on lateral friction since on one hand there is an instantaneous tangent and on the other the superelevation rate is zero. Regarding the continuous superelevation rotation rate approach, at the same breakpoint the vehicle experiences motion from positive to negative superelevation, and since this point is located at an instantaneous tangent, the difference in friction demand is twice the supperelevation rate of the point. For the given values, by utilizing Equation 4 and Equation 8 the demanded lateral friction difference results to:

$$\Delta f_R = 2x2.49/100 = 0.05 \quad (9)$$

The model also classifies the demanded lateral friction in terms of the most critical wheel, where as expected, this wheel was located on the front axle (FWD vehicle). It was found that the highest demand of lateral friction was experienced at the inner wheel to the curve. Therefore, for

section 1, critical was the front left wheel, and for section 2 and section 3 the front right respectively.

Finally yet importantly, Figure 4 also illustrates the total demand in friction, between the two examined approaches, as delivered from Equation 7, where more or less the same conclusions are drawn.

However, in order to investigate the most unfavorable case for the continuous superelevation rotation rate approach, the authors performed the same process by setting $\Delta s=\Delta s_{min}$. Following the same process for EKL 3 design class the relevant parameters were determined (R was set to 300m, A_1 was set to R/3=100m, A_2 was determined 179.00m and e_{L1}, e_{L2} referring to both circular curves were set to 7.0%).

The findings are shown through Figure 5, where additionally the longitudinal friction (f_T) is also shown. As a general conclusion there seems to be (an expected) greater difference in the demanded lateral friction, which results to:

$$\Delta f_R = 2x3.67/100 = 0.07 \qquad (10)$$

It is important to stress the fact that both assessments were performed for the maximum control grade value of 6.50%. The reason is that the longitudinal friction increases with positive grades, thus necessitating greater composite friction. However, for both cases this total friction was found to be below the available unfavorable value of f_{max}= 0.30.

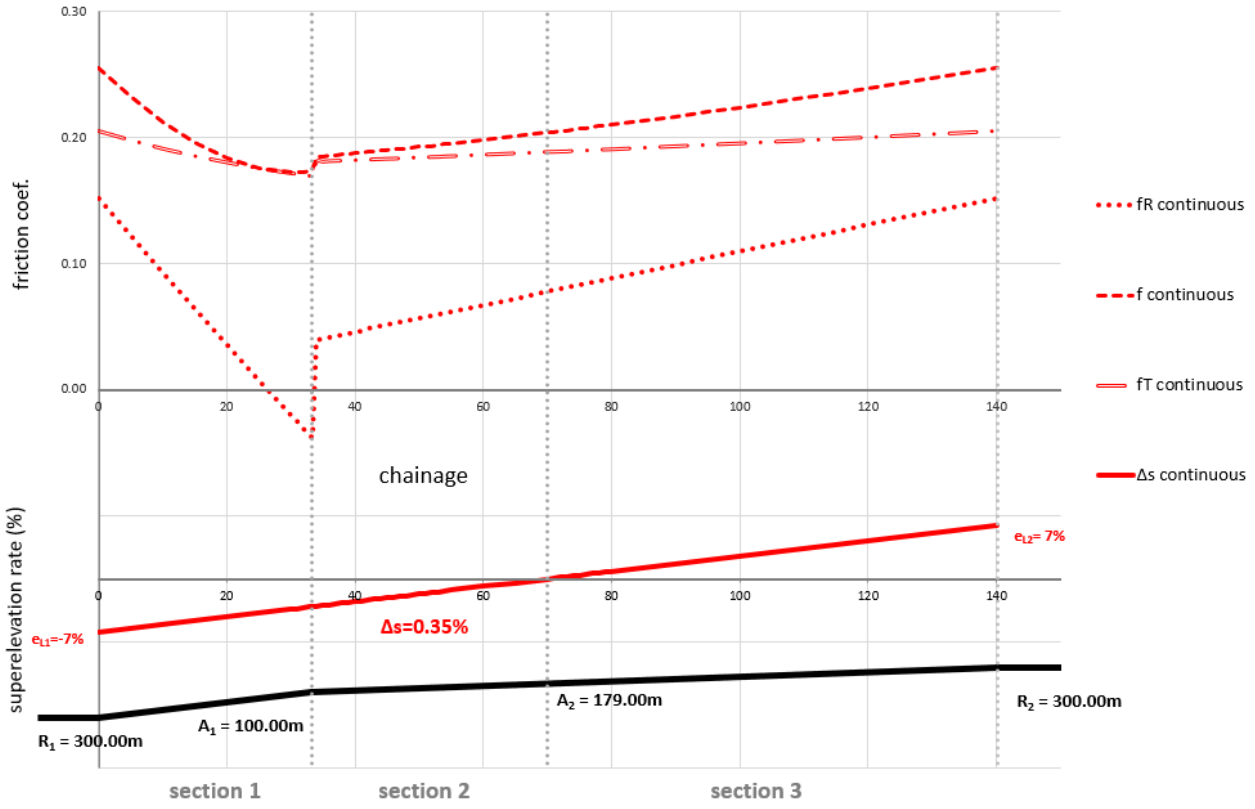

Figure 5 Demanded Side Friction Values (f_R) for the Continuous Superelevation Rotation Rate Approach (case examined: $\Delta s=\Delta s_{min}$)

DISCUSSION AND CONCLUSIONS

The present paper examined the potential of introducing a more flexible and construction-friendly process for accommodating the superelevation rotation rate for arrangements of consecutive reverse curves.

More specifically, an investigation was carried out regarding the impact of generalizing a continuous superelevation transition (rotation rate) between the points where the first circular curve ends and the second circular curve begins against the existing approach according to which the superelevation transition is formed through a breakpoint at the point of reverse curvature (level superelevation, e=0).

The assessment was performed based on the German RAL, 2012 design guidelines, with respect to control values of superelevation and superelevation rotation rates, tailored for cases with high superelevation demand (sharp curves). As a result, the EKL 3 design class was utilized, which refers to vehicle speed value of 90km/h.

Moreover, an existing vehicle dynamics model was also utilized in order to calculate the friction demand for both approaches and quantify the safety effects.

The available friction was set to 0.30 in order to address wet pavements with poor friction performance. Since, during vehicle cornering, the portion of friction experienced in the longitudinal direction, is engaged by the friction demanded laterally, the model calculated the demanded friction portions in both directions of travel, as well as the overall friction, where the available friction was found sufficient for the examined parameters.

Between the two assessed cases and around the point where the alignment changes the curvature direction (left to right or opposite), regarding the demanded lateral friction of the continuous superelevation transition, certain interesting findings were reported. By examining conditions under which the negative superelevation rate is maximized at the instantaneous tangent between the reverse spirals, and at the same time sustain the superelevation rotation rate to the control value of Δs_{min}=0.35%, the results, at that point, revealed that the vehicle undergoes an immediate but rather moderate lateral friction demand variation. This lateral friction difference, was found 0.05 and 0.07 when Δs_{min} was utilized on the conventional and continuous superelevation transition approach respectively.

However, before introducing the proposed approach in road design practice, there are certain issues that necessitate further research.

The present assessment needs to be validated also for speed values beyond the design speed and by investigating the acceleration - deceleration impact, especially braking (14).

In addition, since only a single passenger car was examined, further work is required to incorporate the entire vehicle fleet (SUVs, sport vehicles, heavy vehicles, etc.) as well as their related parameters.

Concluding, it should not be ignored that the human factor during the acceleration process might impose additional restrictions and, consequently, affect vehicle's safety performance.

AUTHOR CONTRIBUTIONS

The authors confirm contribution to the paper as follows: study conception and design: SM, VM; literature collection: SM, VM, SV, KA, GY; review and synthesizing: SM, VM, SV, KA, GY; draft paper preparation: SM, VM. All authors reviewed the results and approved the final version of the manuscript.

REFERENCES

1. American Association of State Highway and Transportation Officials (AASHTO). *A Policy on Geometric Design of Highways and Streets*, Fifth Edition. Washington, DC., 2018.

2. Ed.German Road and Transportation Research Association, Committee, Geometric Design Standards. *Guidelines for the Design of Rural Roads, (RAL),* Germany, 2012.

3. Ministero delle Infrastrutture e dei Trasporti. *Norme Funzionali e Geometriche per la Costruzione delle Strade, n. 6792*, Italy, 2001.

4. Ministry of Environment, Regional Planning and Public Works. *Guidelines for the Design of Road Projects (OMOE-X), Alignment, Part 3*, Greece, 2001.

5. Mavromatis, S., E. Papadimitriou, G. Yannis and B. Psarianos. Vehicle Skidding Assessment through Maximum Attainable Constant Speed Investigation. *Journal of Transportation Engineering, American Society of Civil Engineers Part A: Systems*, Vol.143, Issue 9, ISSN 2473-2907, 2017.

6. Mavromatis, S. A. Laiou, G. Yannis. Safety Assessment of Control Design Parameters through Vehicle Dynamics Model. Accident Analysis and Prevention. AAP491, Vol.125, 2019, pp.344-351.

7. Mavromatis, S., A. Laiou, G. Yannis, B. Psarianos, Acceleration Impact Investigation for Control Road Geometry Parameters. *97thAnnual Meeting of the Transportation Research Board*, Washington, DC., 2018.

8. Gillespie T.D. Fundamentals of Vehicle Dynamics. *Society of Mining Metallurgy and Exploration* Inc.1992.

9. Dixon J.C., Tires, Suspension and Handling. Second Edition. *Society of Autimotive Engineers, Inc Warrendale,* Pa., United Kingdom 1996.

10. Heisler H. Advanced Vehicle Technology. *Edward Arnold. A Division of Hobber & Stoughton*, Germany 1993.

11. Harwood, D. W. and J. M. Mason. Horizontal Curve Design for Passenger Cars and Trucks. *Transportation Research Record 1445*, Transportation Research Board, Washington, DC., 1994, pp. 22-33.

12. Edwards, C. H. Jr & Penney, D. E. Differential Equations and Boundary Value Problems: Computing and Modeling, Prentice-Hall, New Jersey, 1996.

13. Gauss F. Skid Resistance Properties of Tires and their Influence on Vehicle Control In Skidding Accidents. *Transportation Research Board 621, TRB, National Research Council*, pp.8-18, Washington DC., 1976.

14. Torbic, D. et al. NCHRP Report 774: Superelevation Criteria for Sharp Horizontal Curves on Steep Grades. Transportation Research Board, Washington, DC., 2014.